Version 8, June 18th 2006

Limits on the high-energy gamma and neutrino fluxes from the SGR 1806-20 giant flare of December 27th, 2004 with the AMANDA-II detector

The IceCube Collaboration*

(Dated: June 19, 2006)

On December 27th 2004, a giant γ-flare from the Soft Gamma-ray Repeater 1806-20 saturated many satellite gamma-ray detectors. This event was by more than two orders of magnitude the brightest cosmic transient ever observed. If the gamma emission extends up to TeV energies with a hard power law energy spectrum, photo-produced muons could be observed in surface and underground arrays. Moreover, high-energy neutrinos could have been produced during the SGR giant flare if there were substantial baryonic outflow from the magnetar. These high-energy neutrinos would have also produced muons in an underground array. AMANDA-II was used to search for downgoing muons indicative of high-energy gammas and/or neutrinos. The data revealed no significant signal. Upper limits on the normalization constant of the gamma flux were determined for different spectral indices γ. For $\gamma = -1.47$ (-2), the limit is 0.05 (0.5) TeV^{-1} m^{-2} s^{-1} at 90% CL. Similarly, we set limits on the normalization constant of the high-energy neutrino emission of 0.4 (6.0) TeV^{-1} m^{-2} s^{-1} for $\gamma = -1.47$ (-2).

PACS numbers: 95.55.Vj, 95.55.Ka, 95.85.Pw

I. INTRODUCTION

Soft Gamma-ray Repeaters (SGRs) are X-ray pulsars which have quiescent soft (2-10 keV) periodic X-ray emissions with periods ranging from 5 to 10 s and luminosities of the order of 10^{33-35} erg/s. They exhibit repetitive bursts lasting ~ 0.1 s which reach peak luminosities of $\sim 10^{41}$ erg/s in X-rays and γ-rays. There are four known SGRs, three in the Milky Way (including SGR 1860-20) and one in the Large Magellanic Cloud. Three of the four known SGRs have had hard spectrum ($\sim$MeV energy) giant flares with luminosities reaching up to $\sim 10^{47}$ erg/s. The first of these giant flares (from SGR 0525-66 [1]) was observed on March 5, 1979 by the Venera 11 and 12 spacecraft. SGR 1900+14 exhibited a giant flare in 1998 [1]. The most recent and brightest flare came from SGR 1806-20 on Dec. 27, 2004. This flare lasted about 5 minutes, had a peak luminosity of $\sim 2 \cdot 10^{47}$ erg/s and a total energy emission of $\sim 5 \cdot 10^{46}$ erg [2]. This event was observed by several satellite experiments [3–5], although they saturated during the blast. Recent estimates locate the source at a distance of $15.1^{+1.8}_{-1.3}$ kpc [6], but this value is still under debate [7].

The favored "magnetar" model for these objects is a neutron star with a huge magnetic field ($B \sim 10^{15}$ G). These giant flares can be explained as global crustal fractures due to magnetic field rearrangements liberating a high flux of X-rays and γ-rays [8].

During the flare, the γ-ray spectrum up to ~ 1 MeV is well described with a blackbody spectrum with $kT = 175$ keV [2]. However, fits to the data favor the presence of a non-thermal component. Fits using a blackbody + power law (BB+PL) spectrum show that the PL spectral index hardens during the giant flare up to values of the order of $-1.3 \div -1.4$ [2].

The possibility of using underground detectors to observe the muons produced in the electromagnetic showers induced by TeV gammas generated in these flares was presented in Ref. [9]. There have been suggestions of substantial baryonic outflow and the possibility of high-energy neutrino production. Radio observations [10, 11] indicate an expanding radio source with velocity 0.25-0.40c. Gelfand *et al.* [12] argue that a re-brightening of the radio emissions $\sim$20 days after the giant flare can be explained if substantial amounts of released energy went into a baryonic fireball, and make predictions for TeV neutrino production. Ioka *et al.* [13] also argue that high-energy neutrino production can be related to the fraction of burst energy released in the form of baryons.

The Dec. 2004 giant flare represents an excellent opportunity to probe the high-energy spectrum of these sources by looking for events correlated in time and space with this flare. In this paper we present the results of a search for a gamma and/or neutrino signal during the SGR 1806-20 giant flare using data from the AMANDA-II detector. The short duration of these events and the fact that they come from a point-like source result in negligible atmospheric muon and neutrino backgrounds. For the first time, we used down-going muons to look for muon photo-production in the atmosphere, already proposed in Ref. [14]. A search for coincidences using gravitational waves was presented in Ref. [15].

AMANDA (Antarctic Muon and Neutrino Detector Array) is currently running in its AMANDA-II configuration of a 3D array of 677 optical modules (OMs) distributed along 19 strings deployed at depths of 1500-2000 m in the South Pole ice [16]. These 8-inch photomultipliers, enclosed in pressure-resistant glass spheres,

*Corresponding author: J.D. Zornoza, zornoza@icecube.wisc.edu

make it possible to reconstruct direction and energy of relativistic muons through timing and intensity of the Cherenkov light. The ice layer above the detector reduces the background of atmopheric muons by more than 5 orders of magnitude compared to the surface flux. Events are recorded when at least 24 OMs register a signal within 2 μsec. The detector rate on December 27th was 90 Hz (close to the AMANDA-II average).

II. ANALYSIS TECHNIQUE

For events like the burst of the SGR 1806-20 in Dec. 2004, in which most of the energy emitted during the flare is concentrated in a 1 s time scale, the precise time and location of the event imply that the background of atmotspheric muons becomes negligible [9], thereby allowing a search for TeV γ-rays and downgoing TeV neutrinos.

The AMANDA collaboration follows a policy of blindness in its analysis strategies. By studying the expected backgrounds and signals prior to look at the data, the analysis can be designed in an unbiased fashion. In the case of expected small signals, this is particularly relevant for having a clear procedure to determine the probability of an event to be produced by background. Thus, in this analysis, the determination of the optimum selection criteria is done using the simulation of the signal and comparing it with the expected background. The procedure is as follows:

- the background on-source and off-time is calculated using real data, keeping blind 10 min around the burst onset. About one day of off-time data was used to monitor the stability of the detector (see Sec. IV);
- the signal from the source is simulated in order to estimate the angular resolution and the effective area of the detector;
- the appropriate time window is estimated, based on the flare onset times given by different X-ray satellites and their counting rates;
- the optimum search bin size is found by minimizing the Model Discovery Factor (MDF), defined as

$$MDF = \frac{\mu(n_b, CL, SP)}{n_s} \qquad (1)$$

  where μ is the Poisson mean of the number of signal events which would result in rejection of the background hypothesis, at the chosen confidence level CL, in $SP\%$ of equivalent measurements. SP stands for statistical power and n_s is the number of signal events predicted by the model. This definition is analogous to the Model Rejection Factor (MRF see Ref. [17]) that is used for setting upper limits. In the case of the MDF, the bin size is optimized to maximize the probability of discovery (for CL corresponding to five sigma and SP=90%).
- once the optimum search bin size has been found, the unblinding of the data is done, i.e. the events inside the time window and the search bin are counted;
- this number of events is translated into a flux or a flux limit if no significant excess on top of the background is found through the knowledge of the expected signal in the detector for the given analysis cuts.

Although both TeV γ-rays and neutrinos produce muons in the detector array, the optimal choice of selection criteria depends on the assumed signal. The analysis was optimized to the TeV γ signal. Any further optimization to the neutrino signal would be more than offset by the penalty for an additional trials factor.

III. DATA AND SIMULATION

In order to have a background estimate for the flare, a time and angular window have to be defined around the flare of equatorial coordinates (J2000) Right Ascension = 18h 08m 39.34s and Declination = -20° 24' 39.7" [10, 18, 19]. The bulk of the flare energy was concentrated in less than 0.6 s. The SWIFT-BAT counting rate drops by more than 2 order of magnitudes after 0.6 s from the onset of the burst [20]. Based on the observation time for each satellite [3, 5, 15, 21–23], and accounting for its position, the expected signal time in AMANDA was calculated. The spread of the resulting times indicate that a safe window is 1.5 s around 21h 30m 26.6s of Dec. 27th.

To evaluate the performance of the detector, simulations were performed for several input signals. The CORSIKA-QGSJet01 [24] and ANIS [25] codes were used to simulate the photon and neutrino interactions, respectively. The generated energy for photons is 10 TeV to 10^5 TeV and for protons is 10 GeV to 10^5 TeV. The muons were propagated in the ice with MMC [26] and the program AMASIM [27] simulated the response of the detector. The tracks were reconstructed with the same iterative log-likelihood fitting procedure that was applied to the real data.

The angular resolution for different cuts has been studied using the simulation of down-going muons generated by cosmic rays. The angular resolution, defined as the median of the angular difference between the true and the reconstructed track, is 3.5°. This value was obtained using atmospheric down-going muon high statistic simulations and it was checked that this result is robust within 0.1 deg for the expected signals of photons and neutrino induced muons. We also considered a variety of spectral indices for the γ-ray spectrum assuming values given

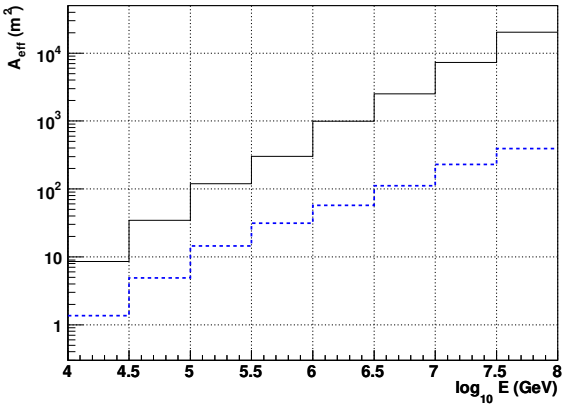

FIG. 1: Effective area after reconstruction and track quality selection for gammas (solid, black) and neutrinos (blue, dashed).

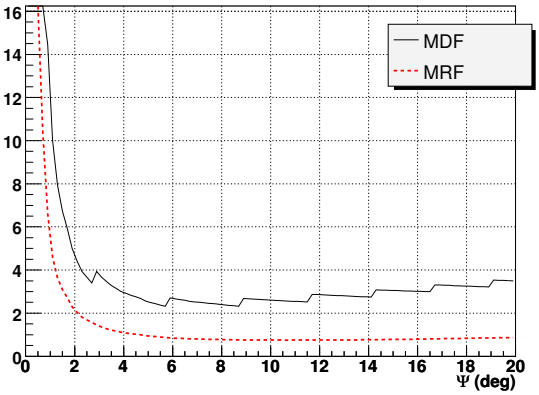

FIG. 2: Model discovery factor (solid, black) and model rejection factor (dashed, red) for an $E^{-1.47}$ spectrum.

in Ref. [9] and we found that the angular resolution is almost independent of the spectral index. The effective areas, defined as the equivalent area for a perfect detector that is able to detect particles with 100% efficiency, for gammas and neutrinos are shown in figure 1 as a function of the energy.

As has been explained before, the optimum angular window is determined by minimizing the Model discovery factor. In figure 2 we show the dependence of the MDF and MRF on the circular angular window around the source position. The steps in the MDF curve are due to the discreteness of Poisson statistics. It can also be seen that the MRF minimum interval is quite broad, indicating that this variable is not very sensitive to the increase in the number of background events with the increase of the angular window. This is due to the small value of the background in the allowed time window.

The search bin size which optimizes the probability of discovery is at 5.8°. With this cut and a 1.5 s time window, the expected background is 0.06 counts. For events that satisfy the detector trigger, we keep almost 80% of the signal in this angular window.

IV. SYSTEMATIC UNCERTAINTIES

Several sources of systematic uncertainties have been considered in this analysis. There is a 20% of uncertainty in the detector efficiency. The uncertainty of the hadronic model calculation is estimated to about 15%, mostly due to the unknown fraction of diffractive ρ production [29]. Moreover, we find a 5% difference when we compare the results using CORSIKA-QGSJET01 and the analytical formulae in [14]. Other uncertainty sources are the overall sensitivity of the OMs (10%) and the optical properties of the ice (3%). The effect has been estimated simulating different reasonable ice models and OM sensitivities.

The stability of the run was checked in order to exclude possible non-particle events induced by detector electronics. These events are identified by a specific method [28] looking for anomalous values in a set of defined variables. A correction is made for the electronics dead time (17%, which is a typical value in normal runs). Finally, the simulated and measured distributions of an extensive set of variables, like zenith angle, number of hit optical modules, and hit times, were compared in the search of possible anomalies. In all the cases the agreement was within the systematic errors estimated above.

V. RESULTS

Once the optimum search bin size of 5.8° around the source was determined, we unblinded the 1.5 s data around the burst looking for events satisfying the analysis requirements. No event was observed in the on-source, on-time window. Then, we determined the upper limits of the normalization constant A_{90} at a CL of 90% assuming a power-law energy spectrum,

$$\frac{dN}{dE} = A_{90}(E/\mathrm{TeV})^{\gamma} \qquad (2)$$

with a cut-off at 10^5 TeV. These limits are shown in figure 3 together with the sensitivity of the detector.

To give an idea of the impact of these limits on theoretical estimates such as the γ flux extrapolations presented in Ref. [9], for spectral index -1.47 (-2) the limit on the gamma flux normalization constant is 0.05 (0.5) TeV^{-1} m^{-2} s^{-1}. The calculation of this limit using the same energy limits as in Ref. [9] would give 3.3 (33) TeV^{-1} m^{-2} s^{-1}, which rules out spectral indices up to $\gamma \sim -1.5$, but not softer (assuming a maximum gamma energy of 500 TeV). The effect of the attenuation of the gamma flux by the cosmic microwave background

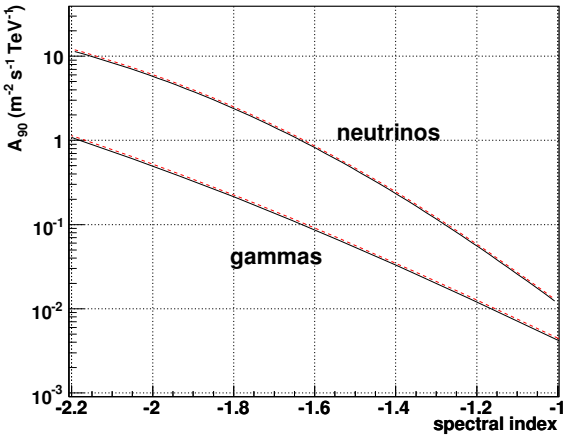

FIG. 3: Sensitivity (dashed, red) and limit (solid, black) to the normalization constant in the flux of gammas (lower, thick line) and neutrinos (upper, thin line), assuming a flux $\phi(E) = A\ (E/\mathrm{TeV})^{\gamma}$.

and the Galactic interstellar radiation field has been also taken into account and has been calculated from the results of Ref. [30].

Since the source is above the horizon (hence there is not much column depth for neutrinos to interact), the neutrino flux limits are an order of magnitude worse than the TeV γ limits, but can still be used to constrain models. In cases where there is large baryonic outflow, high-energy neutrinos are produced and the baryons may make the source partially opaque to high-energy photons. Comparing the extrapolations in Ref. [9], for spectral index -1.47 (-2) the limit on the ν_μ flux normalization is 0.4 (6.0) TeV^{-1} m^{-2} s^{-1} while the model predicts (accounting for oscillations) 1.7 (4.1×10^{-4}) in the same units. We are thus able to exclude an extremely hard neutrino spectrum extrapolated from the measured MeV photon flux. On the other hand, our limit on the high-energy neutrino fluence is still at least one order of magnitude larger than the fluence predicted in Ref. [12].

VI. CONCLUSIONS

In summary, we have searched for TeV gammas and neutrinos associated with the Dec. 27th giant flare from SGR 1806-20 . We demonstrate that underground neutrino arrays such as AMANDA and IceCube can be used as TeV γ detectors for transient events. An analysis of AMANDA data yields no muons coincident with the flare. We use this muon non-observation to place stringent limits on TeV radiation from this source.

[1] C. Barat, *et al.*, Astron. Astrophys. **79**, L24-L25 (1979); T. Cline, E. Mazets, S. Golenetskii, IAU Circ. No.7002 (1998).
[2] P. M. Woods *et al.*, eprint: astro-ph/0602402, subm. to Astrophys. J.
[3] D. Borkowski *et al.*, GCN Circ. **2920**, (2004); S. Mereghetti *et al.*, Astrophys. J. **624**, L105 (2005).
[4] D.M. Palmer *et al.*, GCN Circ. **2925**, (2004).
[5] K. Hurley et al., Nautre. **434**, 1098, (2005).
[6] S. Corbel *et al.*, Astrophys. J. **478**, 624 (1997); S. Corbel and S. S. Eikenberry, Astron. & Astrophys. **419**, 191 (2004).
[7] N. M. McClure-Griffiths and B. M. Gaensler, eprint: astro-ph/0503171.
[8] C. Thompson and R.C. Duncan, *Mon. Not.R. Astron. Soc.* **275**, 255 (1995).
[9] F. Halzen, H. Landsman and T. Montaruli, eprint: astro-ph/0503348 and updated paper in preparation.
[10] P. B. Cameron *et al.*, Nature **434**, 1112 (2005).
[11] B.M. Gaensler *et al.*, Nature **434** 1104.
[12] J.D. Gelfand *et al.*, astro-ph/0503269.
[13] K. Ioka *et al.*. astro-ph/0503279.
[14] M. Drees, F. Halzen and K. Hikasa, Phys. Rev. **D 39**, 1310 (1989); F. Halzen, T. Stanev and G. B. Yodh, Phys. Rev. **D55**, 4475 (1997); F. Halzen and D. Hooper, astro-ph/0305234.
[15] L. Baggio *et al.*, Phys. Rev. Lett. **95**, 081103 (2005).
[16] E. Andrés *et al.*, Astrop. Phys. **13**, 1 (2000).
[17] G.C. Hill and K. Rawlins, Astrop. Phys., **19**, 3, (2003), astro-ph/0209350.
[18] D.L. Kaplan *et al.*, Astrophys. J. **556**, 399 (2001).
[19] K. Hurley, Nature **397**, 41 (1999).
[20] D. M. Palmer *et al.*, Nature **434**, 1107 (2005).
[21] T. Terasawa *et al.*, eprint: astro-ph/0502315, subm. to Nature.
[22] D. Gotz, private communication.
[23] E. Pian and S. Schwartz, private communication.
[24] D. Heck, et al., FZKA-6019.
[25] A. Gazizov and M.P. Kowalski, Comput. Phys. Commun. **172** 203 (2005).
[26] D.A. Chirkin, "Cosmic Ray Energy Spectrum Measurement with the Antarctic Muon and Neutrino Detectro Array", PhD thesis, University of California at Berkeley (2003).
[27] S. Hundertmark "AMASIM Neutrino Detector Simulation Program", Proc. of Simulation and Analysis Methods for Large Neutrino Telescopes, DESY, Zeuthen, Germany, 6-9 July 1998;
[28] A.C. Pohl, "A Statistical Tool for Finding Non-Particle Events from the AMANDA Neutrino Telescope", Licenciat thesis, University of Uppsala (2004).
[29] F. Halzen, K. Hikasa and T. Stanev, Phys. Rev. **D 34**, 2061 (1986);
[30] I. Moskalenko et al., Astrop. J., **640**, 155 (2006).